Hierarchy in Mid-Rapidity Fragmentation: Mass, Isospin, Velocity Correlations

V. Baran, [a] M. Colonna, [b] M. Di Toro [b]

[a] *University of Bucharest, Physics Faculty, and NIPNE-HH Bucharest, Romania*

[b] *Laboratori Nazionali del Sud INFN, I-95123 Catania, Italy*

Physics & Astronomy Dept., Univ. of Catania

Abstract

We present new features of the transition from nuclear multifragmentation to neck fragmentation in semi-central heavy-ion collisions at Fermi energies as obtained within a microscopic transport model, Stochastic Mean Field (SMF). We show that along this transition specific hierarchy phenomena of some kinematic observables associated with the intermediate mass fragments develop. Their correlations with the dynamics of isospin degree of freedom open new possibilities to learn about the density dependence of nuclear symmetry energy below saturation as well as about the fragmentation mechanisms. Detailed results are presented for mass symmetric $Sn+Sn$ reactions with different isospin content at 50 AMeV.

Key words: Nuclear fragmentation, Symmetry energy, Reaction mechanisms

PACS: 25.70.Pq, 25.70.Mn;, 21.65.Ef;, 24.10.Cn

Nucleus-nucleus collisions provide a unique tool to explore the properties of finite interacting fermionic systems in a broad range of densities and temperatures. At energies between 10 and $100A\ MeV$, usually referred to as 'Fermi energies', the mean-field and collisional effects are quite balanced leading to a very intricate dynamics, sensitive to impact parameter and beam energy. Entrance channel effects as well as phenomena well explained in terms of statistical equilibrium can coexist. As a consequence of the two-component character of nuclear matter additionally features due to isospin manifest. Indeed the symmetry energy term in the equation of state (EOS) was one of the main subjects of interest during the last decade [1–3].

The fragmentation process is an ubiquitous phenomenon observed at Fermi energies. However the underlying reaction mechanisms can be rather different and a detailed study can provide independent information on the nuclear EOS out of saturation. Aim of this paper is to suggest new fragment mass-velocity-isospin correlations particularly sensitive to the various mechanisms as well as to the in-medium nuclear interaction.

For central collisions the nuclear multifragmentation can be associated with a liquid-gas phase transition in a composite system [4]. While the final state configurations are well described within statistical equilibrium models [5], but also within hybrid models coupling a dynamical formation and evolution of primary fragments with a secondary decay stage [6], the kinetics of this phase transition can be related to spinodal decomposition in two component nuclear matter [4,7,8] accompanied by the isospin distillation. Increasing the impact parameter the neck fragmentation, with a peculiar intermediate mass fragments (IMF, $3 \leq Z \leq 20$) distribution as well as an entrance channel memory, was observed experimentally [9–12] and predicted by various transport models [13],[14]. In this case the low-density neck region triggers an isospin migration from the higher density regions corresponding to PLF and TLF. Therefore the isospin content of the IMF's is expected to reflect the isospin enrichment of mid-velocity region. For even more peripheral collisions an essentially two-body reaction can by accompanied by a dynamically induced fission of the participants [15,16] and for N/Z asymmetric entrance channel combinations isospin diffusion takes place [17–19].

Consequently the isospin degree of freedom can be seen as a precious tracer providing additional informations about the physical processes taking place during the evolution of the colliding systems. Moreover from a comparison between the experimental data and theoretical model predictions, isospin dynamics allows to investigate the density and/or temperature dependence of the symmetry energy. More exclusive studies from the new experimental facilities certainly will impose more severe restrictions on various models and parametrization concerning this quantity.

Following these arguments we have investigated new features of the fragmentation mechanism from semi-central to semi-peripheral collisions. We mention that for central collisions a correlation between the N/Z of the fragments and their kinetic energy sensitive to the density behavior of the symmetry energy was recently evidenced in a transport model [20]. The average value of this ratio decreases with the kinetic energy per nucleon and it is asy-EOS dependent in multifragmentation.

An experimental study of internal correlations for the fragmentation of quasiprojectiles was performed by Colin el al. [21] within the INDRA collaboration. For certain classes of events a hierarchy of mass fragments along the beam axis was interpreted in terms of the breakup of the very elongated structure resulting from the interaction of the two colliding nuclei, see also [22] for recent results.

In this paper we explore the kinematical properties of the fragments produced at the transition from multifragmentation to neck fragmentation. A hierarchy in the transverse velocity of IMF's is clearly evidenced. Moreover, new interesting correlations between kinematical features of the fragments and isospin dynamics which can provide clues in searching for the most sensitive observables to the symmetry energy are discussed.

We employ a microscopic transport model, Stochastic Mean Field (SMF), based on Boltzmann-Nordheim-Vlasov (BNV) equation [23]. Our choice is motivated by the requirement to have a well implemented nuclear mean-field dynamics together with the effects of fluctuations induced by two-body scattering, as experimental indications at energies between 20 AMeV and 100 AMeV including the behavior of collective flows, suggest that mean-field plays an essential role in shaping the evolution of the system. Within the Stochastic Mean-Field model the time evolution of the one-body distribution function $f(\mathbf{r},\mathbf{p},t)$ is described by a Boltzmann-Langevin equation [24]:

$$\frac{\partial f}{\partial t} + \frac{\mathbf{p}}{m}\frac{\partial f}{\partial \mathbf{r}} + \frac{\partial U}{\partial \mathbf{r}}\frac{\partial f}{\partial \mathbf{p}} = I_{coll}[f] + \delta I[f] \qquad (1)$$

where the fluctuating term $\delta I[f]$ is implemented through stochastic spatial density fluctuations [25]. The collision integral $I_{coll}[f]$ for fermionic systems takes into account the energy, angular and isospin dependent free nucleon-nucleon cross sections. The symmetry energy effects were studied by employing two different density parametrizations [26] of the mean field:

$$U_q = A\frac{\rho}{\rho_0} + B(\frac{\rho}{\rho_0})^{\alpha+1} + C(\rho)\frac{\rho_n-\rho_p}{\rho_0}\tau_q + \\ + \frac{1}{2}\frac{\partial C}{\partial \rho}\frac{(\rho_n-\rho_p)^2}{\rho_0} \qquad (2)$$

where $q = n,p$ and $\tau_n = 1, \tau_p = -1$. For asysoft EOS, $\frac{C(\rho)}{\rho_0} = 482 - 1638\rho$, the symmetry energy $E_{sym}^{pot} = \frac{1}{2}C(\rho)\frac{\rho}{\rho_0}$ has a weak density dependence close to the saturation, being almost flat around ρ_0. For superasystiff case, $\frac{C(\rho)}{\rho_0} = \frac{32}{\rho_0}\frac{2\rho}{\rho+\rho_0}$, the symmetry energy is quickly decreasing for densities below normal density. The coefficients A, B and the exponent α, characterizing the isoscalar part of the mean-field, are fixed requiring that the saturation properties of symmetric nuclear matter with a compressibility around $215MeV$ are reproduced.

A comparative study of the reactions $^{132}Sn + ^{132}Sn$ (EE system), $^{124}Sn + ^{124}Sn$ (HH) and $^{112}Sn + ^{112}Sn$ (LL) at $50MeV/A$, intensively analyzed in the recent years at MSU [17], is performed. We shall focus at the value of impact parameter $b = 4fm$ for which a typical behavior corresponding to the transition from multifragmentation to neck fragmentation, a process not very much investigated up to now, is clearly noted in our simulations. Indeed our previous results indicate at $b = 4fm$ a memory of entrance channel, through the existence of well defined PLF's and TLF's, even if the multiplicity of intermediate mass fragments is still quite large [23]. Therefore, along this transition region, for impact parameters

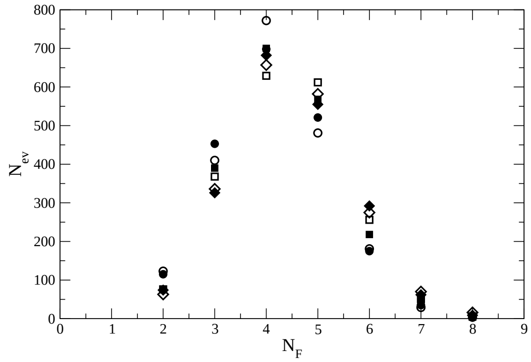

Fig. 1. Fragment multiplicity distribution at $b = 4fm$. Circles:$^{112}Sn +^{112} Sn$. Squares:$^{124}Sn +^{124} Sn$. Diamonds $^{132}Sn +^{132} Sn$. The filled symbols:asysoft EOS. The open symbols:asysuperstiff EOS.

between $3fm$ and $5fm$, a mixing of features associated to multifragmentation and neck fragmentation are expected. The relative values of interaction time scale, of the time scale associated to fragment formation and growth as well as the typical time scales for isospin migration and distillation will determine the properties of emitted IMF's. Consequently a good sensitivity to the symmetry energy density dependence can be expected. At $b = 6fm$ the reaction mechanism corresponds to a neck fragmentation with mostly two or three IMF's observed in the mid-rapidity region and a short nucleus-nucleus interaction time [23].

A total number of 2000 events is generated for each entrance channel combination and equation of state. We adopt an analysis method of kinematical properties which was previously employed in studies concerning dynamical fission or neck fragmentation mechanisms [27,28]. After the freeze-out time, corresponding to the saturation of the number of formed IMF's, we propagate the Coulomb trajectories of all fragments until a configuration where the Coulomb interaction becomes negligible. The asymptotic velocities of PLF and TLF define an intrinsic axis of the event by the vector $\mathbf{V_r} = \mathbf{V}(H_1) - \mathbf{V}(H_2)$ always oriented from the second heaviest fragment H_2 towards the heaviest one H_1. Even for mass symmetric entrance channels this is an appropriate definition when searching for the correlations between kinematic properties of the IMF's and the break-up of the initial composite system. The IMF's of each event are ordered in mass and their orthogonal and parallel components of the asymptotic velocities with respect to the intrinsic axis, together with their charge, are determined. The events are classified accordingly to the number of observed IMF's at freeze-out time. We report in Fig. 1 the multiplicity distributions associated to all studied cases. We select the classes with three and four IMF's, corresponding to around 550 events and 250 events out of the total of 2000 events, providing so a reasonable statistics. In Figure 2 for the events with three IMF's and all entrance channel combinations, HH, EE and LL respectively, the charge distributions corresponding to each order in the mass hierachy are shown. In the following for all figures, always the hystograms brighten as the rank of IMF increases.

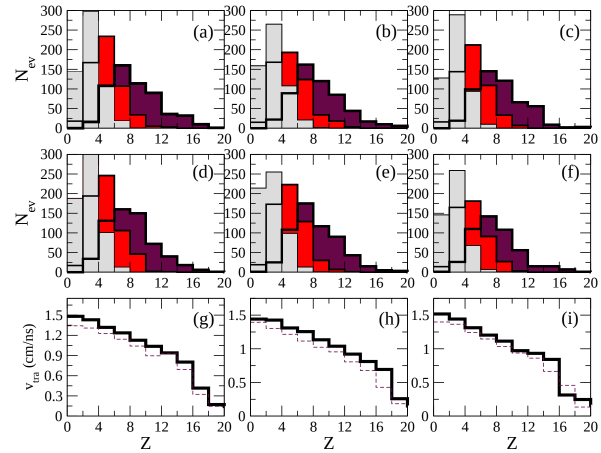

Fig. 2. The charge distribution of the each IMF in hierarchy for asysoft EOS (upper row) and asysuperstiff EOS (middle row). HH combination:(a),(d),(g). EE combination:(b),(e),(h). LL combination:(c),(f),(i). Average transverse velocity distribution as a function of charge (bottom row) for asysoft EOS (thick-solid line) and asysuperstiff EOS (thin-dashed line). All results refer to events with IMF multiplicity three. The hystograms brighten as the rank of IMF's increases.

The heaviest IMF (the rank one in hierarchy) can have a charge up to $Z = 16 - 18$ with distribution centered around $Z = 6 - 8$ while the lightest arrives up to $Z = 8$. In the bottom row the average transverse velocity in each charge bin is calculated considering the contribution of all fragments independent of the position in hierarchy (see Figure 2 (g), (h) and (i)). The transverse velocity has a steep decreasing trend with the charge in agreement with previous findings reported in [29], not much depending on the asy-EOS. In fact this appears to be a general feature of the fragmentation dynamics. The larger transverse velocity of the lightest fragments seems to indicate a reduced driving effect of the PLF, TLF "spectators" i.e. a reduced alignment along the PLF-TLF axis. All that can be related to the presence of a multifragmenting source located in the overlap region upon which the shape instabili-

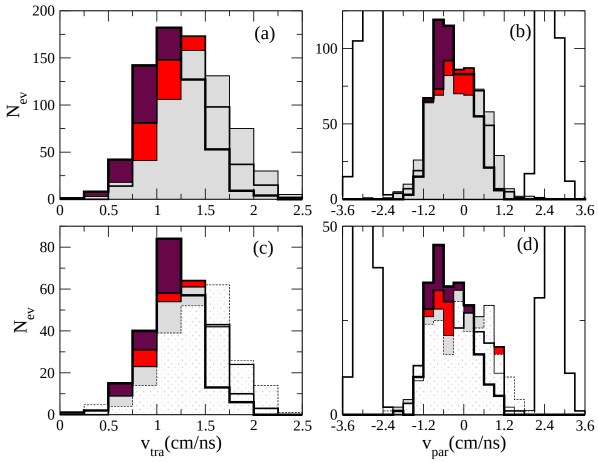

Fig. 3. HH combination in the asysoft EOS choice. Upper panels: fragmentation events with three IMF. (a) Transverse velocity v_{tra} distributions, (b) Parallel velocity v_{par} distributions. Bottom panels: events with four IMF. (c) v_{tra} distributions, (d) v_{par} distributions. The hystograms brighten as the rank of IMF increases.

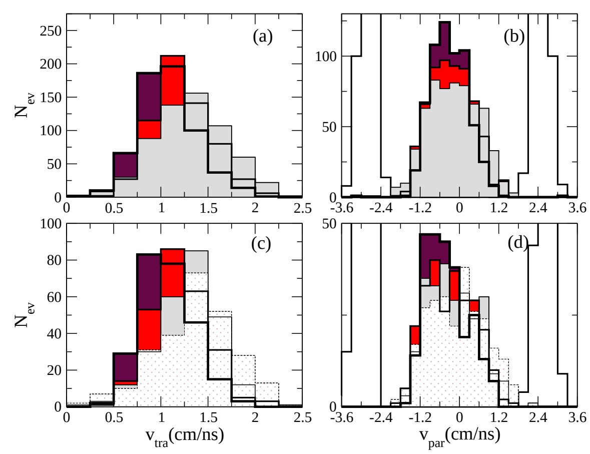

Fig. 4. Like Fig.3, in the asysuperstiff EOS choice.

ties of the neck dynamics will take over.

In the following, we discuss more in detail the kinematical properties of fragments, once ordered in mass. The correlations between velocity and size are amplified when analyzing the events according to the fragment rank in the hierarchy.

In Figures 3 and 4 for asysoft and superasystiff EOS respectively, we report the IMF's transverse and parallel velocity distributions in the case of HH combination. We also plot the parallel velocity distributions of projectile and target like residues.

For both classes of events the transverse velocity distribution shifts towards higher values with the position in the mass hierarchy, the lightest fragment acquiring highest v_{tra}. This hierarchy in the veloc-

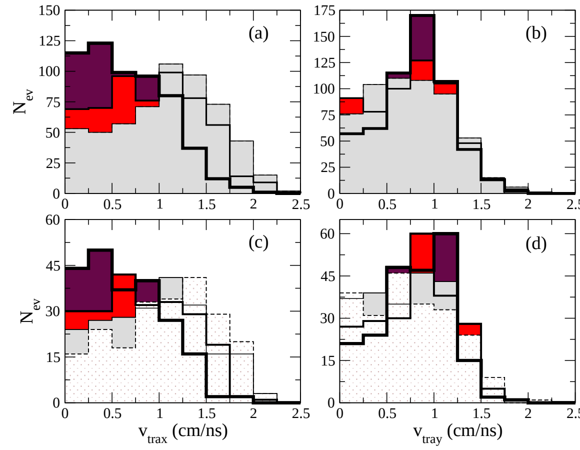

Fig. 5. The asysoft EOS and HH combination. Transverse velocity in reaction plane, v_{trax}, distribution for fragmentation events with three IMF (a) and four IMF respectively (c). Transverse velocity out of reaction plane, v_{tray}, distribution out of reaction plane for fragmentation events with three IMF (b) and four IMF respectively (d).

ity perpendicular to the intrinsic axis emerges as a specific signal characterizing the transition from multifragmentation to neck fragmentation. It can be related to the peculiar geometrical configuration of the overlapping region and its fast evolution. The velocity distributions along the intrinsic axis are centered around mid-velocity region, quite decoupled from the PLF and TLF. This is analogous to what is observed in neck fragmentation. We stress that it is likely to exist some other production mechanisms not described by our transport model, including breakup or fission of strongly deformed quasiprojectile/quasitargets, which take place on longer time scales. We notice that while in most of the events the heaviest IMF is anti-correlated with the lightest among PLF and TLF residues, there are cases when this is not manifest. The parallel velocity distribution of the lightest IMF looks broader and more symmetric around the center of mass velocity, suggesting a dominant volume contribution of spinodal and thermal nature to the fragment formation like in multifragmentation. However it is difficult to notice any hierarchy in the IMF velocity along the intrinsic axis.

The transverse velocity distribution has been analyzed more in detail, by looking separately at in reaction plane and out of reaction plane components, see Fig. 5. The observed hierarchy seems to be influenced by the behavior of the in reaction plane transverse velocity. The presence of a transverse collective flow, larger for the lightest masses in the hier-

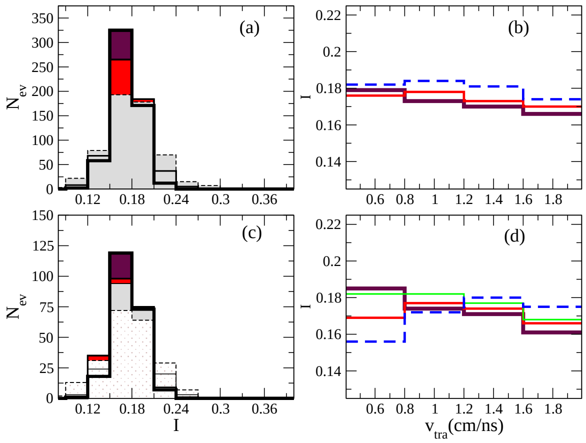

Fig. 6. HH combination in the asysoft EOS choice. Upper panels: events with three IMF. (a) Isospin distributions;(b) Fragment isospin content vs transverse velocity. Bottom panels:events with four IMF. (c) Isospin distributions;(d) Fragment isospin content vs transverse velocity. All histograms are like in the caption of Fig. 3. The dashed lines correspond to the ligthest IMF. A thinner continuous line is associated with a lighter IMF.

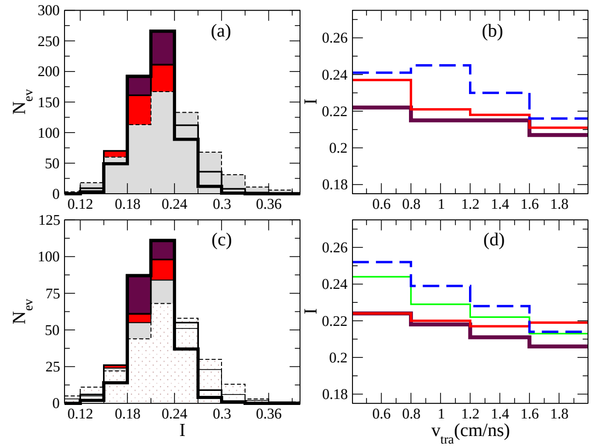

Fig. 7. Like in Fig.6, in the asysuperstiff EOS choice.

archy, is clearly evidenced by the shift of the peak in the velocity distributions pointing towards an incomplete dissipation of entrance channel collective energy. The out of reaction plane transverse velocity distributions are less extended reflecting the thermal fluctuations and larger Coulomb effects for the heaviest IMF.

In spite of this, when the two components are combined to form the final distributions in transverse velocity, the hierarchy is still rather evident, see Figs. 3,4. This suggest that essential is the measure of the rate at which the fragments departs from the intrinsic axis and this depends on their rank in mass hierarchy.

As already noted the features discussed above are determined mainly by the isoscalar part of the equation of state. On top of that the symmetry energy induces various changes on the properties related to the isospin content of the fragments. We have extended our investigations to isospin observables studying their dependence on the IMF position in hierarchy as well the correlation to transverse velocity. In Figures 6, (for asysoft EOS) and 7 (for asysuperstiff EOS) we report the asymmetry $I = (N-Z)/(N+Z)$ distribution of each IMF of the hierarchy. The results refers again to HH system whose initial asymmetry is $I = 0.194$.

Several differences between the two asy-EOS are evidenced. For asysoft EOS the isospin distributions are centered at a lower value and their widths are rather narrow. At variance, for asysuperstiff EOS the centroids of the distributions are closer to the initial value of the composite system and their broader widths depend on the position in the mass hierarchy. For both asy-EOS the lightest IMF's are more likely to acquire higher values of the asymmetry. We also notice that similar results were obtained for the other entrance channel combinations, LL and EE respectively.

We relate these features to the differences between the two asy-EOS at sub-saturation densities. Clearly, a larger value of the symmetry energy will fasten the isospin distillation process and all IMF's reach lower and closer values of the asymmetry. This is the case for the asysoft EOS. On the other hand larger values of fragment asymmetry in the case of asysuperstiff EOS shows that this was not very effective during the formation phase.

The fragments grow in quite low density, more asymmetric regions, as a result of isospin migration. The differences inside the hierarchy for the latter asy-EOS point towards different formation time scales with the lightest IMF finding more neutron rich environment and a distillation process not fast enough to produce the same symmetry for all IMF's in the event. However it is interesting to remark that these fragments also acquires the largest transverse velocity as it was discussed before. Therefore a possible scenario is that they escape faster from the active region keeping a partial memory of the early conditions of the fragmentation. At variance if they have lower transverse velocity, appearing in a richer neutron region will carry higher asymmetry. We represent the average asymmetry as a function of transverse velocity in figures 6 for asysoft EOS and 7 for asysuperstiff EOS.

A decreasing trend is generally observed for the IMF's, more pronounced for asysuperstiff EOS. Moreover, in the latter case, the trend is particularly evident for the lightest IMF's, in agreement with the previous discussion.

For a given transverse velocity bin the asymmetry always increases with the rank in hierarchy in the case of asysuperstiff EOS. On the other hand, in the case of the asysoft EOS we cannot appreciate much such differences, all fragments reaching almost the same asymmetry.

A similar analysis has been carried out for the LL combination aiming to construct isospin double ratios and study their dependence on the transverse velocities. Concerning the fragment isotopic content, similar differences between the two asy-EOS, as observed for the HH combination, were evidenced, in spite of the fact that Coulomb effects are now more important. We also obtained a similar dependence of the fragment asymmetry on the transverse velocity. Therefore the double ratios do not show appreciable differences between the two asy-EOS. The same conclusion was reached in central collisions [20]. However, as we noticed before, different trends can be detected, within the same system, between fragments belonging to different ranks in hierarchy, especially in the superasystiff case.

In conclusion in this letter by employing a microscopic transport model we evidenced new features of nuclear fragmentation in semi-central to semipheripheral collisions.

At Fermi energies an almost continuous transition with the centrality is revealed, from multifragmentation to neck fragmentation mechanisms. Good observable tracers appears to be related to the correlations between the fragment masses,transverse velocities and isospin contents. In fact specific hierarchy phenomena are signaled: the distributions of the velocity perpendicular to the intrinsic axis of the event depend on the rank in a mass hierarchy of the event. In the reaction plane the lightest fragments acquire greater transverse velocities, phenomenon observed for several mass entrance channels. This feature can be used as an identification of the fragmentation mechanism discussed in this paper.

Another important finding is that the fragment isospin content is sensitive to the position in this hierarchy and this can be related to the density dependence of symmetry energy at sub-saturation densities as well as to the relative time scales for fragment formation and isospin transport.

These observations open new opportunities from the experimental point of view. An analysis of isospin dependent observables in correlation to position in mass hierarchy or kinematic observables may add more constrains on the behavior of symmetry energy below normal density and may provide a supplementary support for the assumption that the IMF's form in the low density regions of heated nuclear matter. We mention that recent experimental results reported by CHIMERA collaboration for the system $Sn + Ni$ at a lower energy ($35AMeV$) [30] sustain the existence of the hierarchy in transverse velocity as discussed in this paper. Their analysis also signaled differences in the isospin content of IMF's when ordered in a mass hierarchy, the lightest fragments being more asymmetric. This kind of observations support an asystiff-like behavior of the symmetry energy at sub-saturation densities.

Aknowledgements

The authors are grateful to E. De Filippo,A. Pagano, P. Russotto, and CHIMERA Collaboration for stimulating discussions. One of authors, V. B. thanks for warm hospitality at Laboratori Nazionali del Sud. This work was supported in part by the Romanian Ministery for Education and Research under the CNCSIS contract PN II ID-1038/2008.

References

[1] V. Baran, M. Colonna, M. Di Toro, V. Greco, Phys. Rep. 410 (2005) 335.

[2] A.W. Steiner,M. Prakash,J.M. Lattimer, P.J. Ellis Phys. Rep. 411 (2005) 325.

[3] Bao-An Li, Lie-Wen Chen, Che-Ming Ko, Phys. Rep.464 (2008) 113.

[4] P. Chomaz, M. Colonna, J. Randrup, Phys. Rep. 389 (2004) 263.

[5] A.H. Raduta, M. Colonna, M. Di Toro, Phys. Rev. C76 (2007) 024602.

[6] J. Frankland et al., Nucl. Phys. A 689 (2001) 940; B. Borderie et al., Phys. Rev. Lett. 86 (2001) 3252.

[7] V. Baran, M. Colonna, M. Di Toro, A.B. Larionov, Nucl. Phys. A 632 (1998) 287.

[8] V. Baran, M. Colonna, M. Di Toro, V. Greco, Phys. Rev. Lett. 86 (2001) 4492.

[9] E. De Filippo et al., Phys. Rev. C 71 (2005) 044602.

[10] M. Di Toro, A. Olmi, R. Roy, Eur. Phys. J. A 30 (2006) 65.

[11] P. Milazzo et al., Nucl. Phys. A 703 (2002) 466.

[12] P. Russotto et al. (Chimera Coll.), Phys. Rev. C 81 (2010) 064606.

[13] V. Baran, M. Colonna, M. Di Toro, Nucl. Phys. A 730 (2004) 329.

[14] M. Papa et al., Phys. Rev. C 75 (2007) 054616.

[15] E. De Filippo et al., Phys. Rev. C 71 (2005) 064604.

[16] P. Russotto et al. (Chimera Coll.), Int. J. Mod. Phys. E 15 (2006) 410.
[17] M.B. Tsang et al., Phys. Rev. Lett. 92 (2004) 062701; M.B. Tsang et al., Phys. Rev. Lett.102 (2009) 122701.
[18] V. Baran et al., Phys. Rev. C 72 (2005) 064620.
[19] J. Rizzo et al, Nucl. Phys. A806 (2008) 79.
[20] M. Colonna et al., Phys. Rev. C 78 (2008) 064618.
[21] J. Colin et al. (INDRA Coll.), Phys. Rev. C 67 (2003) 064603.
[22] A.B McIntosh et al., Phys. Rev. C 81 (2010) 034603.
[23] V. Baran et al., Nucl. Phys. A 703 (2002) 603.
[24] J. Rizzo, Ph. Chomaz, M. Colonna, Nucl. Phys. A806 (2008) 40 and refs. therein.
[25] M. Colonna et al., Nucl. Phys. A642 (1998) 449.
[26] M. Colonna, M. Di Toro, G. Fabbri, S. Maccarone, Phys. Rev. C 57 (1998) 1410.
[27] A.A. Stefanini et al. Z. Phys. A 351 (1995) 167.
[28] J. Wilczynski et al, (CHIMERA Coll.) Int. J. Mod. Phys. E 14 (2005) 353.
[29] R. Lionti et al., Phys. Lett. B 625 (2005) 33.
[30] E. De Fillippo et al.(CHIMERA Coll.), Invited talk at IWM 2009, Catania, Italy. SIF Conf. Proceedings vol. 101, Bologna 2010, pg. 178-188.